



Cite this: DOI: 10.1039/c6fo01842d

trans-Polydatin protects the mouse heart against ischemia/reperfusion injury *via* inhibition of the renin–angiotensin system (RAS) and Rho kinase (ROCK) activity†

Dong Ming,^{†a} Liao Songyan,^{‡c,d} Chen Yawen,^a Zheng Na,^a Ma Jing,^a Xiao Zhaowen,^a Liu Ye,^b Ding Wa^a and Liu Jie^{*a}

Background: Recent studies highlighted the protective benefits of a Chinese herb extract from *polygonum cuspidatum*, *trans*-polydatin, on cardiac disease. We investigated the therapeutic effect of *trans*-polydatin on myocardial ischemia/reperfusion (IR) injury and the underlying mechanisms related to the renin–angiotensin system (RAS) and RhoA kinase (ROCK) pathway. **Methods and results:** Experiments were performed on neonatal rats' ventricular myocytes that were subjected to hypoxia–reoxygenation (simulated IR, SIR) and on adult mice which were subjected to left anterior descending coronary artery occlusion for 45 min followed by a one-week reperfusion. *trans*-Polydatin significantly increased cell viability and reduced apoptosis in SIR cardiomyocytes. It was also observed to reduce the infarct size and increase the cardiac function in IR mice. *trans*-Polydatin decreased the expression of angiotensin and inhibited the activities of renin and angiotensin-converting enzyme. Furthermore, *trans*-polydatin inhibited ROCK activity, especially the angiotensin I receptor-activated ROCK pathway. **Conclusions:** *trans*-Polydatin exerts a cardio-protection against myocardial IR injury likely through inhibiting both RAS and the downstream ROCK pathway.

Received 23rd December 2016,
Accepted 10th May 2017

DOI: 10.1039/c6fo01842d

rsc.li/food-function

1. Introduction

Increasing applications of natural products have recently emerged in the field of cardio therapy. *trans*-Polydatin (PD), 3,4',5-trihydroxystilben-3-β-D-mono-D-glucoside, is a natural resveratrol glucoside extracted from the perennial herbage *Polygonum cuspidatum* Sieb. et Zucc.¹ The orally administered *trans*-polydatin is metabolized primarily to resveratrols in the small intestine and liver, where they are further metabolized to glucuronidated resveratrols.² Similar to its resveratrol analogs, PD participates in multiple biological activities of cardiovascular and hematological systems, including anti-inflammation, anti-oxidation, lipid synthesis reduction, and promotion of microcirculation. The cardio-protection of PD may involve the activation

of cNOS, which leads to an increase in NO production³ and a decrease in apoptosis.⁴ It enhances the heart function, promotes microcirculatory perfusion during shock,⁵ and increases the survival rate during severe shock.⁶ Experimental evidence has shown that PD protects cardiomyocytes from ischemia and ischemia-reperfusion injury.^{3,7} However, the beneficial effect of PD on cardiac IR injury and the underlying mechanisms are poorly understood.

Cardiac IR injury is known to stimulate the renin–angiotensin system (RAS), including the local tissue RAS in the ischemic myocardium and the circulating RAS.⁸ Components of the RAS, such as angiotensinogen, renin, angiotensin-converting enzyme (ACE), angiotensins, and angiotensin receptors, are activated during acute myocardial infarction and the post-infarction remodeling process.^{8–10} Particularly, the increased angiotensin II (Ang II) is a principle effector which binds to Ang II type 1 (AT1) receptors exerting deleterious effects on heart metabolism and functions. Thus, various heart dysfunctions like arrhythmias, suppression of contractility, alterations in energy metabolism, and cardiac fibrosis develop. The underlying mechanisms include but are not limited to activation of the intracellular signaling Janus kinase/signal transducer, generation of increased reactive oxygen species (ROS), disturbance of Ca²⁺ homeostasis, and

^aMedical College, Shenzhen University, Shenzhen, Guangdong 518000, China.
E-mail: ljljz@yahoo.com; Fax: +86 75586671906

^bDepartment of Anatomy, Hebei Medical University, Hebei 050017, China

^cDivision of Pathophysiology, Medical College, Shenzhen University, Shenzhen, Guangdong, China

^dCollege of Optoelectronic Engineering, Shenzhen University, Shenzhen, Guangdong, China

†Electronic supplementary information (ESI) available. See DOI: 10.1039/c6fo01842d

‡Co-first authors.

mitochondrial dysfunction. Interestingly, many studies have demonstrated that the binding of Ang II to its receptors activates the Rho/Rho-kinase (ROCK) pathway which has recently been proved to play an active role during cardiac IR injury.¹¹ The active AT1R and AT2R target at different parts of ROCK signaling, exerting detrimental or protective effects. Recently, the activation of AT2R has been reported to cause RhoA phosphorylation at ser188, which partially counteracts the detrimental effect of ROCK activation after IR injury.¹² Moreover, due to the critical role of the RAS, AT1R blockers (ARB) and ACE inhibitors (ACEi) have been applied as cornerstones in therapy for cardiac IR injury.^{13,14} Early initiation and long-term administration of ACEi are recommended in all major guidelines to treat patients with left ventricular systolic dysfunction and heart failure due to myocardial infarction. However, both ARB and ACEi have side effects. ARB may cause uncontrolled Ang II concentration that results potentially in hypotension and increases in creatinine and potassium levels; ACEi may induce coughing, rashes, taste disturbance, and angioedema.¹⁵ Thus, new agents (drugs) with multiple targets at the RAS and its downstream signals but causing few side effects are highly in demand.

In this study, we hypothesized that PD exerts a cardio-protective function against IR injury by inhibiting the activated RAS and its downstream signals. To test this hypothesis, we examined the effects of PD on various components of the RAS both in cultured neonatal rats' cardiomyocytes that were subjected to simulated IR (SIR, *i.e.*, hypoxia/reoxygenation) injury and in mice which were subjected to left anterior descending coronary artery occlusion and reperfusion. Furthermore, we investigated the influence of PD on the RhoA/ROCK signaling pathway. We expected to find PD improving cardiac function both *in vitro* and *in vivo* after IR injury. The cardio-protective effect of PD is thought to be associated with inhibitions of both the RAS and its downstream RhoA/ROCK signaling pathway.

2. Materials and methods

2.1 Drugs and reagents

trans-Polydatin (with a purity of 98.87%) was supplied by Haiwang Co. (Shenzhen, Guangdong, China). The ROCK inactivates myosin phosphatases *via* a specific phosphorylation of myosin phosphatase target subunit 1 (MBS or MYPT1) at Thr-853, which increases phosphorylated contents of the 20 kDa myosin light chain (MLC20). Therefore, in this study, following the most common method for ROCK activity measurement, the ROCK activity was measured as the ratio of pMBS to MBS. Primary monoclonal antibodies for western blotting and immunostaining and their sources are listed as follows: anti-myosin phosphatase target subunit-1 (MYPT-1), phosphor T853-MYPT1, phospho-RhoA (ser-188), and angiotensin 1/2 receptor (AT1/2) were all from Santa Cruz Biotechnology; angiotensinogen and angiotensin I-II were both from Abcam; and β -actin was from Sigma (all diluted: 1:1000). Masson's trichrome kit Sigma HT15-1KT was used in the study.

Angiotensin-converting enzyme inhibitor (ACEi) (enalapril) was obtained from Sigma (E9658).

2.2 Cell culture

All animal experiments were performed in accordance with the ethical standard as formulated in the Guide for the Care and Use of Laboratory Animals published by the U.S. National Institutes of Health (NIH Publication 85-23, revised 1996) and were approved by the Institutional Animal Care and Use Committee of Shenzhen University. Neonatal cardiomyocytes were isolated and cultured using a previously described method.¹⁶ Cardiomyocytes were used in experiments only when they showed beating and formed a confluent monolayer in synchrony after 72 hours. To simulate ischemia reperfusion heart injury, myocytes were then treated with 1% O₂ for 2 hours in non-glucose culture media and placed under normal conditions for 4 hours.

The C_{\max} of polydatin in the plasma is from 10 $\mu\text{g ml}^{-1}$ (25 μM) to 20 $\mu\text{g ml}^{-1}$ (50 μM) for humans (data from Haiwang company, phase 2 clinical stage), so we used 30 and 50 μM as the working concentrations *in vitro*. Polydatin was added before one hour of IR treatment.

2.3 MTT analysis

Cell viability was assessed using the Vybrant MTT cell Proliferation Assay Kit (Invitrogen) as previously described.¹⁷ The absorbance at 570 nm was measured for experimental groups using a plate reader.

2.4 Mitochondrial membrane potential ($\Delta\psi$) analysis

Cells were seeded onto small glass slides (Orange Scientific, E.U.). JC-1 assay reagent (25 $\mu\text{mol L}^{-1}$) (Bi yuntian, Beijing) was diluted with the dilution buffer (500 μL per well). The diluted reagent was then added to cells and incubated at 37 °C for 20 min to stain the mitochondria. After 2 to 3 rinses with wash buffer, the cells were inspected using an Axiovert 200 fluorescence inverted microscope (Zeiss, Germany). Both monomers (excitation at 488 nm, emission 500–550 nm) and aggregations (excitation 488 nm, emission at 575–620 nm) were registered using the microscope. In each slide, about 200 cells were counted to confirm a visible and comparable result.

2.5 Western blotting

The total protein was measured with a bicinchoninic acid assay kit (Pierce) after sonication of ischemic/reperfused myocardial tissues and harvested cells. Protein components were separated on 7.5% polyacrylamide gels, transferred onto nitrocellulose paper, and stained with primary and secondary antibodies. Reactive bands were visualized by using the Supersignal ECL western blotting detection kit (Pierce), and densitometry was performed *via* the ImageJ software.

2.6 ELISA analysis of angiotensin converting enzyme (ACE) and measurement of renin activity

The activity of angiotensin converting enzyme (ACE) was determined by spectrofluorometry using Z-phenyl-L-histidyl-L-

leucine (Bachem Bioscience Inc) as the substrate and it is expressed in units per milliliter (1 unit = 1 nmol of L-histidyl-L-leucine formed per minute).¹⁸ A radioimmunoassay (RIA) was designed to measure the renin activity of the rats' neonatal myocardiocytes *in vitro* and of the circulating plasma *in vivo* by the quantitation of the generated Ang I.¹⁹

2.7 Animals

Ten-week-old C57BL/6 male mice (20–22 g) were supplied by the animal center of Shenzhen Medical University. All animal care and experimental procedures were performed in accordance with institutional animal ethical committee guidelines. The IR model was set up by subjecting mice to left anterior descending coronary artery (LAD) occlusion for 45 min followed by a 24 h reperfusion. The surgical procedures were performed as previously described.^{20,21} The qualified result was verified by regional cyanosis of the myocardium and changes of the typical electrocardiogram (ECG).²² The experimental flow chart was included (Fig. 1A). *trans*-Polydatin (50 mg kg⁻¹ d⁻¹,¹⁶ dissolved in saline) and the vehicle were orally administered to experimental (I/R + PD) and positive control (sham) mice respectively 24 hours after surgery. Cardiac function and myocardial infarct size were examined 8 days after surgery. The experiments were performed on mice with non-diseased hearts and no abnormal ECG appeared. Unless accidental

death occurred due to anesthesia or surgical failures, the number of mice in each group was recorded (sham: *n* = 15; I/R: *n* = 20; and I/R + PD (50 mg kg⁻¹): *n* = 17).

2.8 Infarct size

At the end of the study, all of the mice were sacrificed by an overdose of sodium pentobarbital. The area at risk (AAR), infarct size, and viable area were evaluated as previously described *via* Evans blue/2,3,5-triphenyltetrazolium chloride (TTC) staining.²³ Briefly, the non-ischemia areas were indicated by Evans blue staining. The infarct size was determined by the size of white stains in the heart. The ischemic but viable tissues were stained with TTC as red color. The AAR was determined by the areas of white with red. All stained areas were measured by computerized video planimetry (Adobe Photo-shop, version 5.5). According to the area-based method, the area of the infarcted region and/or AAR were recorded as a percentage of the total area of the slide.

2.9 Cardiac function

Cardiac function was evaluated after 45 min coronary artery occlusion and 8-day reperfusion. Mice were anesthetized with 2% isoflurane and placed in a supine position on a heated platform. The chest and abdomen were shaved. The extremities were fixed to electrodes on the platform surface with tape

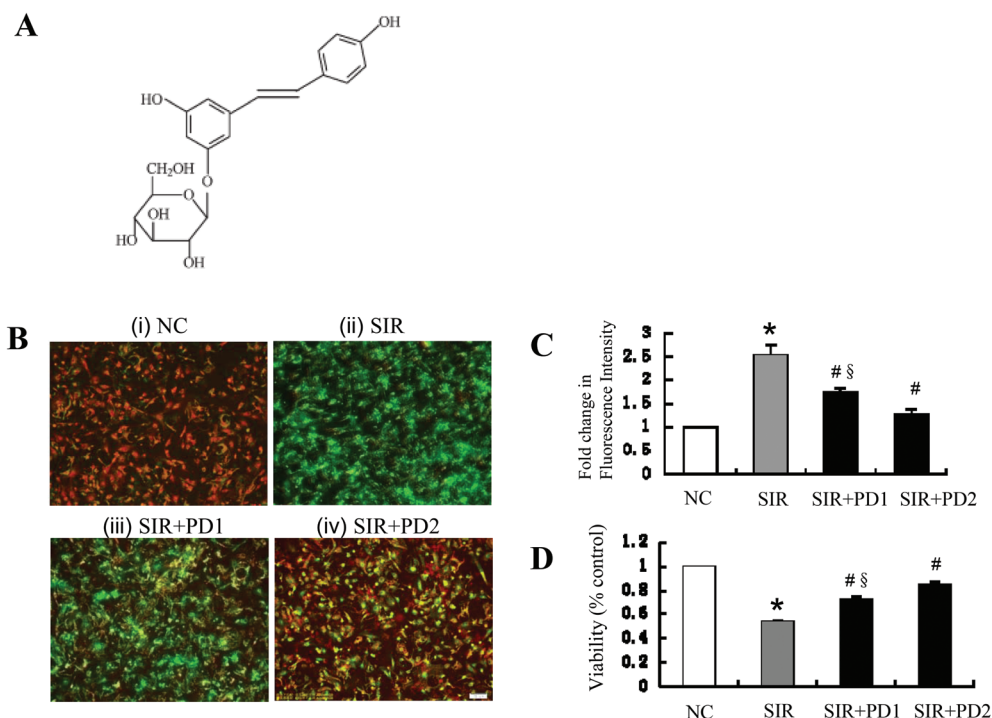


Fig. 1 PD attenuated apoptosis and increased viability in neonatal cardiomyocytes subjected to stimulated ischemia-reperfusion (SIR) injury. **A**. The chemical structure of *trans*-polydatin. **B**. The representative images of neonatal cardiomyocytes stained with JC-1 after SIR injury with or without PD treatment. SIR caused mitochondrial membrane potential ($\Delta\psi(m)$) reduction in cells (green fluorescence increase) whereas PD treatment increased SIR reduced the $\Delta\psi(m)$ production (green fluorescence decrease). (i) Control cells, (ii) cells with SIR injury, (iii) PD1 (30 μ M) treated cells and (iv) PD2 (50 μ M) treated cells after SIR injury. **C**. Statistics of the mitochondrial membrane potential of neonatal cardiomyocytes in different groups. Results expressed as mean \pm SD; *n* = 8. NC: normal control; SIR, simulated ischemia-reperfusion; PD: *trans*-polydatin. **D**. Cell viability by MTT assay in different groups (*n* = 20). **p* < 0.05 vs. normal control (NC), # *p* < 0.05 vs. SIR injury, §*p* < 0.05 vs. NC.

and the highly conductive electrode gel. Echocardiography evaluations were performed using a Vevo 2100 high-resolution *in vivo* micro-imaging system equipped with a real-time micro-visualization scan head of 17.5 MHz (VisualSonics, Toronto, Ontario, Canada). M-mode 2-dimensional echocardiography images were obtained from the parasternal short axis. Images were analyzed using the Vevo 2100 Protocol-Based Measurements software. All measurements were done from the leading edge to the leading edge according to the American Society of Echocardiography guidelines.

2.10 Masson trichrome and tunnel staining

Histopathology of the sections from the myocardial tissue was performed after 45 min ischemia and 8-day reperfusion. To assess the condition of myocardial fibrosis, the pathological collagen deposition on each Masson's trichrome-stained section (HT15, Sigma) was measured using the microscope. The ratio of the fibrotic area to the total area of the left ventricular myocardium was calculated and analyzed for each heart. The apoptotic myocytes were detected by terminal deoxy-nucleotidyl transferase mediated dUTP nick end-labeling (TUNEL) assay using a Cell Death Detection Kit (Roche) according to the manufacturer's instructions as described previously.²⁴

2.11 Statistical analysis

All data were recorded as mean \pm standard division. Differences between two groups were evaluated using unpaired Student's *t* test. One-way ANOVA was conducted for multiple comparisons. Both tests were followed by a *post hoc* Student–Newman–Keuls test when necessary. All analyses were carried out using SPSS 17.0 (SPSS, Chicago, IL), and $p < 0.05$ was considered to be statistically significant.

3. Results

3.1 *trans*-Polydatin protected cardiomyocytes from simulated ischemia-reperfusion (SIR) injury

To simulate ischemia-reperfusion (SIR) injury, cultured neonatal rat ventricular myocytes (NRVMs) were subjected to hypoxia–re-oxygenation. We examined the effect of PD on cellular apoptosis of cardiomyocytes subjected to SIR injury by using a cationic and voltage-sensitive vital fluorochrome (JC-1) and measuring the mitochondrial membrane potential ($\Delta\psi_m$) *in situ*. In mitochondria with normal $\Delta\psi_m$, JC-1 aggregates to a polymer and emits red fluorescent signals. On the other hand, JC-1 is released into the cytoplasm and emits green fluorescent signals in the damaged mitochondria with depolarized $\Delta\psi_m$. The chemical structure of *trans*-polydatin is shown in Fig. 1A. The cellular damage was indicated by the mitochondrial membrane potential ($\Delta\psi_m$) with a complete disappearance of post-SIR red fluorescent signals (Fig. 1B). However, a relatively stable post-SIR $\Delta\psi_m$ was observed in cardiomyocytes with PD treatment (Fig. 1B and C). Furthermore, the potential effect of PD on the cell viability of NRVMs subjected to SIR was assessed by the MTT assay. We observed that SIR significantly

decreased the cell viability to 56.2% in the control group. Treatments with a PD concentration of 30 and 50 μ M remarkably increased the cell viability by 37.3% and 60.0%, respectively (Fig. 1D). The observations collectively indicate that PD has a protective effect on cardiomyocytes against IR injury.

3.2 *trans*-Polydatin inhibited the renin–angiotensin system (RAS) in cardiomyocytes after SIR injury

We investigated the possible role of the RAS in PD-mediated cardioprotection on cardiomyocytes after IR injury. As a key effector of the RAS, the increased angiotensin (Ang) II expression level in cardiomyocytes suggests the damaging effect of the RAS on the ischemic myocardium. We thus determined angiotensin expression in NRVMs subjected to SIR. Since no available anti-angiotensin antibody distinguishes clearly Ang I and II, we determined the total expression of Ang I and II in this study. Consistent with the previous result, the protein level of Ang I–II was obviously increased in NRVMs after SIR injury (Fig. 2A and B). Surprisingly, PD treatment almost completely eliminated the SIR-induced Ang I–II enrichment.

In RAS signal transduction, angiotensinogen, renin, and ACE are required for the production of Ang II. Angiotensinogen is cleaved by renin to form Ang I, which is then transformed into Ang II by ACE.¹¹ To determine the responsible molecule(s) for PD-induced inhibition of Ang II production after IR injury, we analyzed the contents of angiotensinogen and ACE, as well as the activity of renin in cardiomyocytes. As the ACE is released by ACE secretase on the membrane surface of various cells, we evaluated the ACE concentration in the cultural supernatant to quantify the ACE on the cardiomyocyte membrane. The increased protein level of angiotensinogen in cardiomyocytes was observed after IR injury (Fig. 2A and C). Similarly, the ACE concentration in the cultural supernatant (Fig. 2D) and the activity of renin in cardiomyocytes (Fig. 2E) were both increased. PD treatment decreased the ACE concentration and the renin activity, but further increased the angiotensinogen expression (Fig. 2B–E). The results indicate that PD might decrease the Ang level by inhibiting ACE and rennin activity rather than suppressing angiotensinogen expression. The increase in angiotensinogen with PD treatment might be partially attributed to the decrease in renin activity, which likely inhibited the conversion of angiotensinogen to angiotensin. Moreover, a decreased angiotensin level might cause angiotensinogen to increase as a compensatory response. Similar to PD, we found that enalapril (10 μ M), the angiotensin converting enzyme inhibitor (ACEi), increased the angiotensinogen level in both normal and SIR-injured cardiomyocytes (ESI 1†). Therefore, the unexpected increase in angiotensinogen may also be explained as the result of PD-induced ACE inhibition.

To further confirm that the PD-mediated cardioprotective effect in SIR-stimulated cardiomyocytes is associated with inhibition of the RAS, we treated SIR-injured cells with PD and enalapril (an angiotensin-converting-enzyme (ACE) inhibitor) (10 μ M). Enalapril-only treatment significantly increased cell viability and decreased apoptosis in SIR-stimulated cells (Fig. 2F and

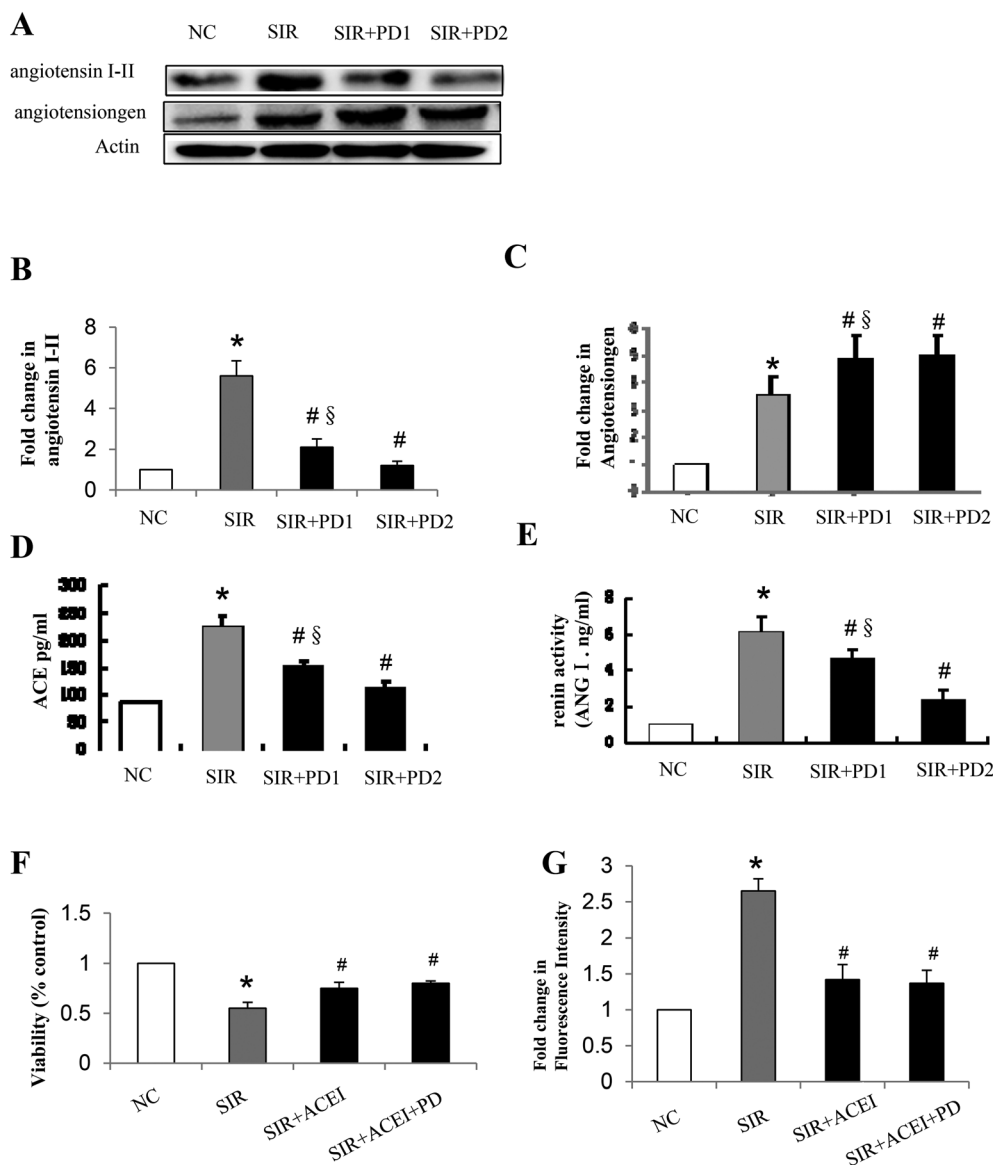


Fig. 2 PD inhibited renin–angiotensin system (RAS) in cardiomyocytes after SIR injury. A. Representative western blotting images of angiotensin (I–II) and angiotensinogen in SIR neonatal cardiomyocytes with or without PD treatment. B, C. Pooled data of the protein levels of angiotensin (I–II, B) and angiotensinogen (C) in different groups. $n = 4$ in each group. D. Expression of ACE in cell supernatant in normal control (NC), SIR injury and PD treatment groups. $n = 4$ in each group. E. Renin activity in different groups. $n = 4$ in each group. Compared with normal control, renin activity in cardiomyocyte is significantly increased after SIR injury and returns to normal with PD treatment, as well as plasma ACE level. F, G. Statistics of the cell viability by using MTT assay (F, $n = 10$ in each group) and mitochondrial membrane potential indexed by JC-1 fluorescence (G) in SIR neonatal cardiomyocytes treated with/without ACEI alone or a combination of ACEI and PD. Data are expressed as mean \pm SD. * $p < 0.01$ vs. NC, # $p < 0.01$ vs. SIR, § $p < 0.05$ vs. NC.

G), suggesting that the activated RAS plays an important role during cardiac IR injury. Treating SIR-stimulated cells simultaneously with PD and enalapril, we found that the cardioprotective effect of PD only slightly increases (Fig. 2F and G). The observations further prove the causal relationship between the inhibition of the RAS and the PD-mediated cardioprotection in IR injury.

3.3 *trans*-Polydatin decreased Rho-kinase (ROCK) activity in SIR-stimulated cardiomyocytes

As RhoA/ROCK activation has a crucial contribution to IR-induced cellular damage,²² in this study, we investigated the

effect of PD on ROCK activity in cardiomyocytes after IR injury. We measured the phosphorylation level of a ROCK substrate MYPT-1 *via* western blotting with anti-T853-phosphorylated MYPT-1 antibody to determine ROCK activity. Consistent with the previous report, ROCK activity was increased to 2.6-fold of normal control after SIR (Fig. 3).²⁵ PD treatment significantly attenuated ROCK activity up to 60% (Fig. 3B). Interestingly, similar to the effect of PD, suppressing the angiotensin production with enalapril (10 μ M) also inhibited ROCK activation in SIR-stimulated cardiomyocytes (Fig. 3C and D). However, no further influence on the protein level of Ang I–II or the ROCK activity was observed in

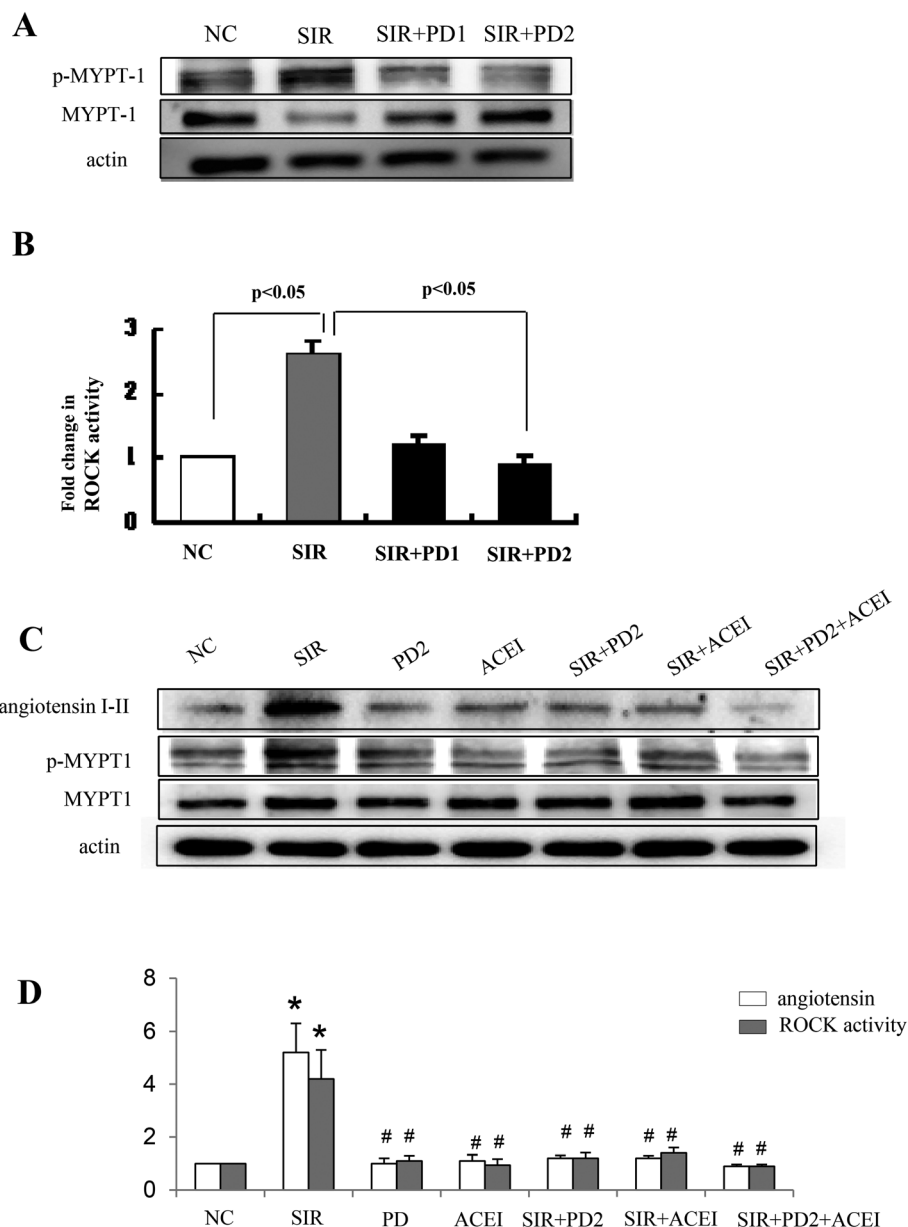


Fig. 3 PD decreased Rho-kinase (ROCK) activity in SIR-stimulated cardiomyocytes. **A**. Representative western blotting bands of p-MYPT-1, total MYPT-1 and β -actin proteins in neonatal cardiomyocytes in normal control, ischemic injury and PD treatment groups. **B**. The densitometric analysis of ROCK activity (p-MYPT-1 divided by MYPT-1) was normalized to β -actin ($n = 10$). **C**. Western blotting bands of angiotensin (I–II), p-MYPT-1, total MYPT-1 and β -actin proteins in neonatal cardiomyocytes in normal control, ischemic injury, PD treatment and ACEi treatment groups. **D**. The densitometric analysis of ROCK activity (p-MYPT-1 divided by MYPT-1) and angiotensin (I–II) protein level ($n = 4$). Data are expressed as mean \pm SD. * $p < 0.05$ vs. normal control (NC), # $p < 0.05$ vs. SIR injury.

the enalapril and PD combining treatment (Fig. 3C and D). The results collectively indicate that the inhibition of the activated RAS by PD is largely responsible for the inhibition of RhoA/ROCK activation by PD in SIR-stimulated cardiomyocytes.

3.4 *trans*-Polydatin dominantly inhibited AT1R-mediated ROCK activation in SIR-stimulated cardiomyocytes

The AT1R-mediated biological activities are detrimental, whereas AT2R is beneficial to cardiac function.¹¹ Both AT1R and AT2R are increased simultaneously after IR injury, and the

AT1R-mediated detrimental effects are dominant.¹¹ Recently, a study made a breakthrough finding distinguishing the AT2R-mediated ROCK signal from AT1R. According to the study, the activation of AT2R results in RhoA phosphorylation at ser188, which partially counteracts the detrimental effect of AT1R-mediated ROCK activation after IR injury.¹² To explore whether PD also exerts cardioprotection at the receptor level, *i.e.*, increasing AT2R function, we firstly examined both expressions of AT1R and AT2R. Consistent with previous studies,^{26,27} both expressions of AT1R and AT2R were

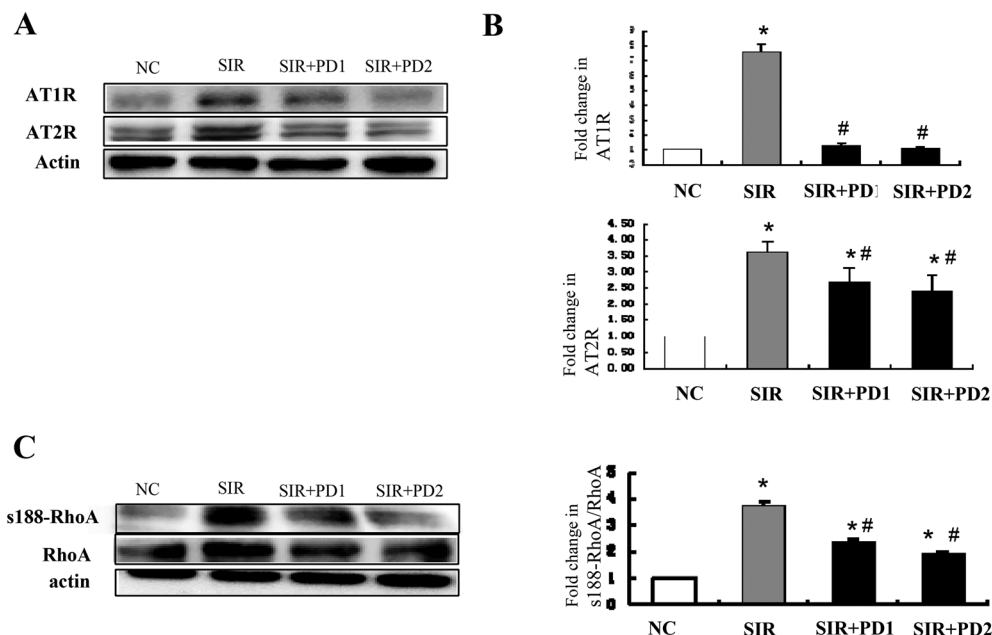


Fig. 4 Effects of PD on the expression of AT1R, AT2R and AT2R-mediated phosphorylation of RhoA (ser-188). A, B. Representative images of western blotting (A) and pooled data (B) of angiotensin receptor type 1 (AT1R) and angiotensin receptor type 2 (AT2R) protein. C. Representative images of western blotting (left) and pooled data (right) of phospho-RhoA (ser-188) and RhoA in neonatal cardiomyocytes under different conditions. Data are expressed as mean \pm SD. $n = 4$ in each group. * $p < 0.05$ vs. normal control (NC), # $p < 0.05$ vs. SIR injury.

increased after SIR (Fig. 4A and B). Both expressions of AT1R and AT2R were decreased with PD treatment. However, the suppression in AT1R by PD was more significant than that on AT2R. The expression of AT1R was decreased by 75%, whereas AT2R was only decreased by 17%. Corresponding to the increase in the AT2R expression of SIR-stimulated cardiomyocytes, phos-RhoA (ser188) was significantly increased (Fig. 4C). Although the level of phos-RhoA (ser188) was reduced with PD treatment, it was still much higher than that of the control (Fig. 4C) ($p < 0.05$). In contrast, after the PD treatment, ROCK activity was suppressed to the same level as that in control (Fig. 3A and B). The results collectively indicate that the inhibition of AT1R signal is dominant to the inhibition of AT2R signal by PD-mediated cardioprotection.

3.5 *trans*-Polydatin decreased infarct size, cardiomyocyte fibrosis, and apoptosis in IR-injured mice

When orally administered to rats, *trans*-polydatin was absorbed rapidly. The results of the non-compartmental pharmacokinetic analysis are shown in Table 1. The therapeutic effect of PD on cardiac IR injury was examined *in vivo* on the IR-injured

mouse model. The representative images of heart sections stained with Evans blue/TTC are shown in Fig. 5B. The area at risk (AAR)/LV ($62 \pm 12\%$ vs. $60 \pm 6\%$) (Fig. 5B) was almost equal in all hearts exposed to IR treatments, indicating similar ratios of ischemic and perfused tissue to the whole heart section among groups. As an index of post-I/R tissue necrosis, the size of the infarcted region was determined and normalized to AAR. *trans*-Polydatin significantly decreased the infarct size/AAR ($81 \pm 14\%$ to $44 \pm 7\%$, $p < 0.05$) after 45 min ischemia followed by 8-day reperfusion (Fig. 5B). The release of the biochemical marker Troponin-T (TnT) into serum was significantly promoted, suggesting that IR injury induced the necrotic cell death of myocytes (Fig. 5C). PD treatment significantly decreased the serum TnT level in IR-injured mice. PD significantly decreased the increased fibrotic area in the heart after IR injury (Fig. 5D). Heart tissue from sham-operated mice exhibited extremely low levels of TUNEL staining (Fig. 5Ea). In contrast, a significantly large amount of TUNEL-positive myocytes was detected on the ischemic myocardial tissue from the hearts subjected to IR injury in the vehicle group (Fig. 5Eb). Notably, the number of TUNEL-positive myocytes of the ischemic myocardium was significantly decreased in PD-treated animals (Fig. 5Ec). Quantitative measurement depicts a 45% reduction in TUNEL-positive myocytes in the *trans*-polydatin-treated group when compared with that in the vehicle group ($n = 5$) (Fig. 5Ed).

3.6 *trans*-Polydatin attenuated the reduction of left ventricular function in mice after IR

The representative echocardiographic M-mode records show that the mice exhibited a pronounced decline in LV wall

Table 1 Main pharmacokinetic parameters of *trans*-polydatin (50 mg kg^{-1}) in rats after oral administration

Parameter	<i>trans</i> -Polydatin (50 mg kg^{-1})
$t_{1/2}$ (min)	115
T_{max} (min)	23
C_{max} (ng mL^{-1})	1100

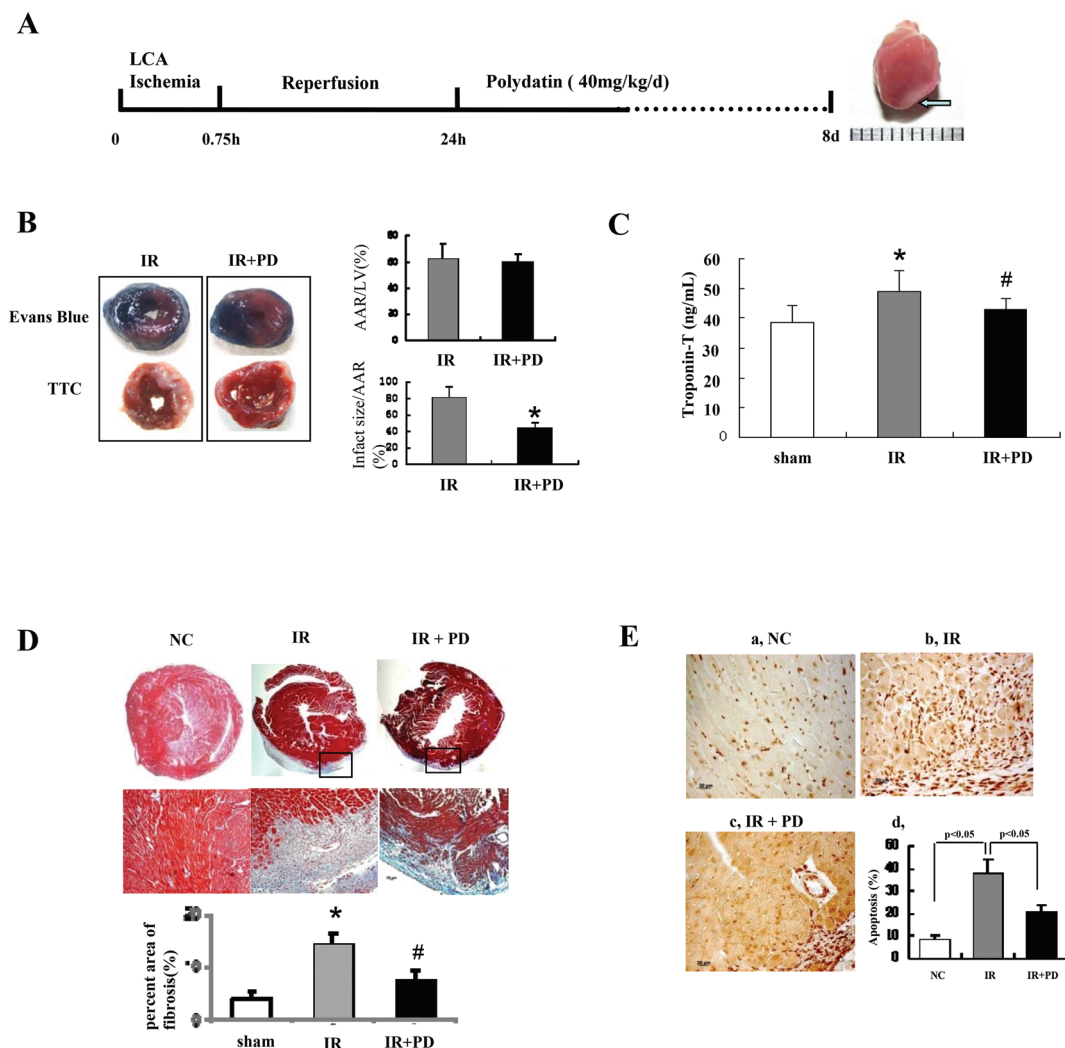


Fig. 5 PD decreased infarct size, cardiomyocyte fibrosis and apoptosis in IR mice. **A.** Experimental flow chart. The IR model was generated by left anterior descending coronary artery (LCA) occlusion for 45 min followed by reperfusion. After 24 hours of the surgery, *trans*-polydatin ($40 \text{ mg kg}^{-1} \text{ d}^{-1}$, dissolved in saline) or vehicle was orally administered. The experimental duration was 8 days. The right heart was taken out after 8 days of IR surgery. The arrow points to the ischemic injury site in the heart. **B.** Representative illustrations of heart sections stained with Evans blue/TTC. The area at risk (AAR) and infarct regions were determined at 8 days after reperfusion. Dark blue stain-viable area; white stain-infarct region; white plus red stain-AAR. The ratio of AAR/LV area (%) was similar between all hearts exposed to IR treatments (upper). The infarct size was normalized to the AAR (%), *trans*-polydatin administration significantly decreased the infarct size (% of AAR) after 45 min ischemia followed by 8 days of reperfusion compared with the IR group (lower). **C.** The average of the serum level of Troponin-T in mice after 7 days to IR. Data are expressed as mean \pm SD. $n = 15$. **D.** Representative images and quantitative analysis of the fibrotic area (Masson trichrome-stained area in light blue normalized to the total myocardial area; magnification, $\times 400$). **E.** Apoptotic cardiomyocytes were identified by TUNEL analysis. TUNEL-positive cells were manifested as a marked appearance of dark brown apoptotic cell nuclei (E, a–c, bar 250 mm). (E, d) Quantitative analysis of percentage of apoptotic cardiomyocytes ($n = 5$). $*p < 0.01$ vs. NC, $\#p < 0.01$ vs. IR. LCA: left anterior descending.

motion on the eighth day after IR and PD treatment preserved it (Fig. 6A). The reduction of left ventricular (LV) function was suggested by an attenuation of the LV wall motion and reductions of the LV ejection fraction (LVEF) and ventricular septum in IR mice (Fig. 6B and C). The result of further analysis demonstrates that *trans*-polydatin treatment restored effectively the LV function (Fig. 6B and C). In the same time, the systolic and diastolic internal diameters were obviously decreased in the polydatin treatment group when compared with the IR group (Fig. 6D and E).

3.7 *trans*-Polydatin inhibited RAS components and ROCK activity in IR-injured mice

We also investigated *in vivo* whether the cardio-protective effect of PD is related to the inhibition of the RAS and RhoA/ROCK signaling pathway as observed *in vitro*. Consistent with the finding *in vitro*, in IR-injured mice, we observed increases in the expressions of angiotensinogen, Ang I-II, AT1R, and AT2R in heart tissue, and increases in the renin activity and ACE concentration of circulating plasma, indicating that IR

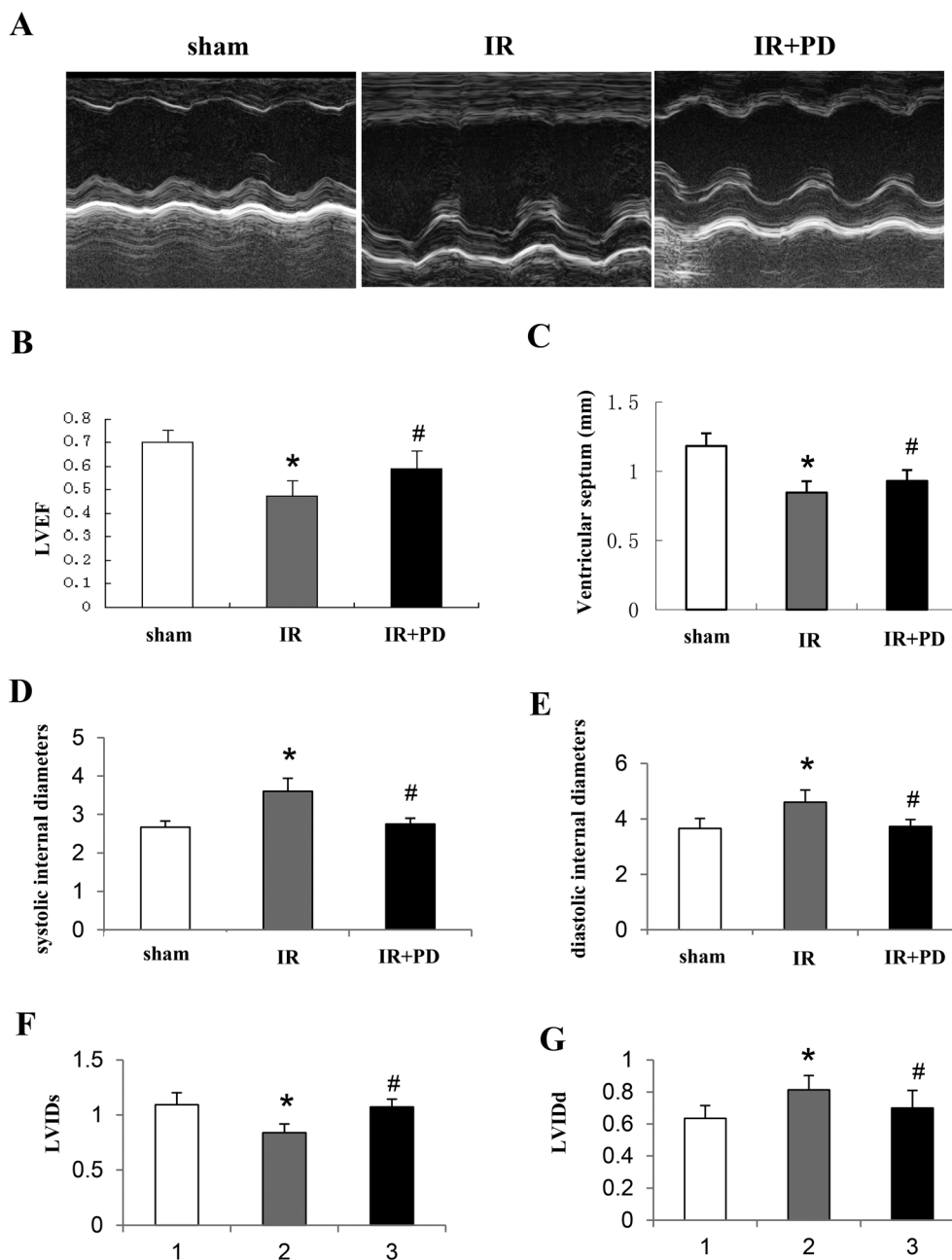


Fig. 6 PD attenuated the reduction of left ventricular function in IR mice. A. Representative echocardiographic M-mode records obtained at the papillary muscle level at 8 days post-IR surgery in mice treated with saline or *trans*-polydatin. B, C. PD significantly increased in the left ventricular ejection fraction (LVEF) and ventricular septum after 8 days of IR surgery. D and E were systolic and diastolic internal diameters. F and G were left ventricular posterior wall (systolic and diastolic). Data are expressed as mean \pm SD. $n = 10$. * $p < 0.01$ vs. NC, # $p < 0.01$ vs. IR.

induced the activation of the RAS (Fig. 7A–C). PD suppressed the expressions of Ang I–II, AT1R, and AT2R, as well as reduced the renin activity and ACE concentration (Fig. 7A–C). Thus, it inhibited effectively the activated RAS components in IR mice. Moreover, IR caused a 2.1-fold increase in phosphorylated MYPT-1 (T853) when compared with the sham-operated heart. PD treatment effectively decreased p-MYPT-1 by 32% (Fig. 7B). The results indicate that PD treatment *in vivo* inhibited RAS and ROCK activations which were induced by IR injury.

4. Discussion

In this study, PD has been proven to reduce the ischemia/reperfusion damage *in vitro* and *in vivo*. PD reduced apoptosis and increased cellular viability in neonatal cardiomyocytes exposed to SIR injury. Moreover, in the IR-injured mouse model of LAD coronary artery occlusion, PD reduced the infarct size, decreased fibrosis and apoptosis in heart tissue, and improved cardiac function. We propose for the first time

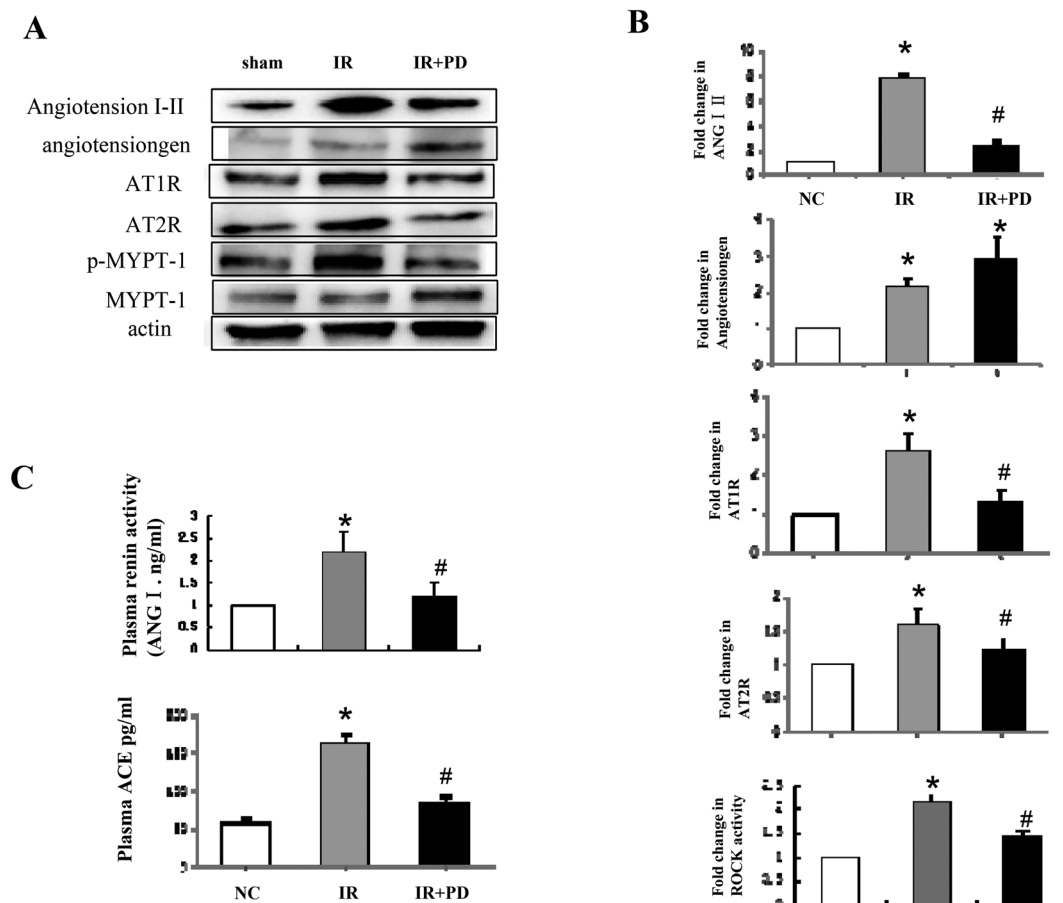


Fig. 7 Effects of PD on myocardial and circulating RAS signaling and myocardial ROCK activation in IR mice. A, B. Representative images of (A) pooled data (B) of western blot of angiotensin I–II ($n = 4$), angiotensinogen ($n = 4$), AT1R ($n = 5$), AT2R ($n = 4$), and ROCK activity ($n = 4$). C. Levels of renin activity and ACE in plasma. Data are expressed as mean \pm SD. * $p < 0.01$ vs. NC, # $p < 0.01$ vs. IR.

that PD suppressed the RAS by targeting on multiple RAS components, which include rennin, ACE, Ang, and the receptors of Ang. Furthermore, we found that the inhibition of the RAS by PD accounts for the PD-induced inhibition of the activated RhoA/ROCK signaling pathway. Notably, PD was observed to mainly suppress the detrimental AT1R-activated ROCK pathway (phos-MYPT-1 at T853), while it meanwhile inhibits less effectively the protective AT2R-activated ROCK pathway (phos-RhoA at ser188).

It has been proven that the RAS is activated and plays a major role in IR cardiac injury.²⁸ In addition to the circulating RAS, the local cardiac RAS has also been found to be up-regulated, and contributes to IR injury and post-IR remodeling.²⁹ In the cascade of the RAS, renin cleaves angiotensinogen to form Ang I. Ang I is then further cleaved by ACE to form Ang II. Ang II is an effector peptide of the system. It stimulates the receptors of AT1R and AT2R, and consequently induces other biological activities. During cardiac IR injury, Ang II exerts damaging effects on cardiac function by inducing AT1R expression. In the past few decades, AT1R blockers (ARB) and ACE inhibitors (ACEi) have been applied as cornerstones in therapy to treat cardiac IR injury. However, ARB and ACEi cause side effects while exerting therapeutic effects. Ang II

reactivation, aldosterone escape, and breakthrough have been observed during ACEi and ARB treatments, and may endanger the clinical benefits of the RAS blockade.³⁰ Thus, novel pharmacological agents and treatments have been increasingly in demand to not only target at multiple components of the RAS cascade but also prevent multiple side effects of ACEi and ARB. The observations of our study proved that PD targeted at multiple components of the RAS and inhibited both the local and circulating RAS after IR injury. Moreover, it inhibited the rennin activity, suppressed ACE and angiotensin, and reduced the expressions of AT1R and AT2R. Therefore, PD may be superior to all available RAS inhibitors, such as ACEi and ARB, in the treatment of cardiac IR injury.

The circulating rennin is expressed and secreted mainly by juxtaglomerular cells.³¹ During cardiac IR injury, increased circulation of rennin may contribute to insufficient renal perfusion. On the other hand, PD has been proved to improve microcirculation, and consequently the ischemia organ function during hemorrhagic shock.⁶ This biological function of PD may at least partially account for the PD-induced inhibition of the circulating RAS. Previous studies have shown that rennin might be released from cardiac mast cells to damage cardiomyocytes *via* paracrine.³² In our recent study, we demon-

strated that PD could act as a mast cell stabilizer,³³ and has therapeutic effects during IR injury, decreasing both circulating and secretory rennin activities. In addition, PD was observed to decrease the local RAS in cardiomyocytes after IR injury. However, the underlying mechanisms of how PD improves the microenvironment and consequently inhibits renin and ACE in cardiomyocytes remain still unknown and require further studies.

In this study, we also found that PD suppressed the activated Rho/ROCK signaling pathway that has been reported to

play an important role during cardiac IR injury. Evidence indicated the causal relationship between the inhibitions of the RAS and RhoA/ROCK pathways by PD treatment. Briefly, ACEi was observed to decrease Angs and inhibit potently ROCK activation after IR injury. Similarly, PD was found to inhibit the angiotensin level and ROCK activity in the cardiomyocytes subjected to IR. No further inhibition in ROCK activity was noticed in the PD and ACEi combined treatment. The binding with either AT1R or AT2R of Ang II has been known to cause ROCK activation. However, recently, activation of AT1R and

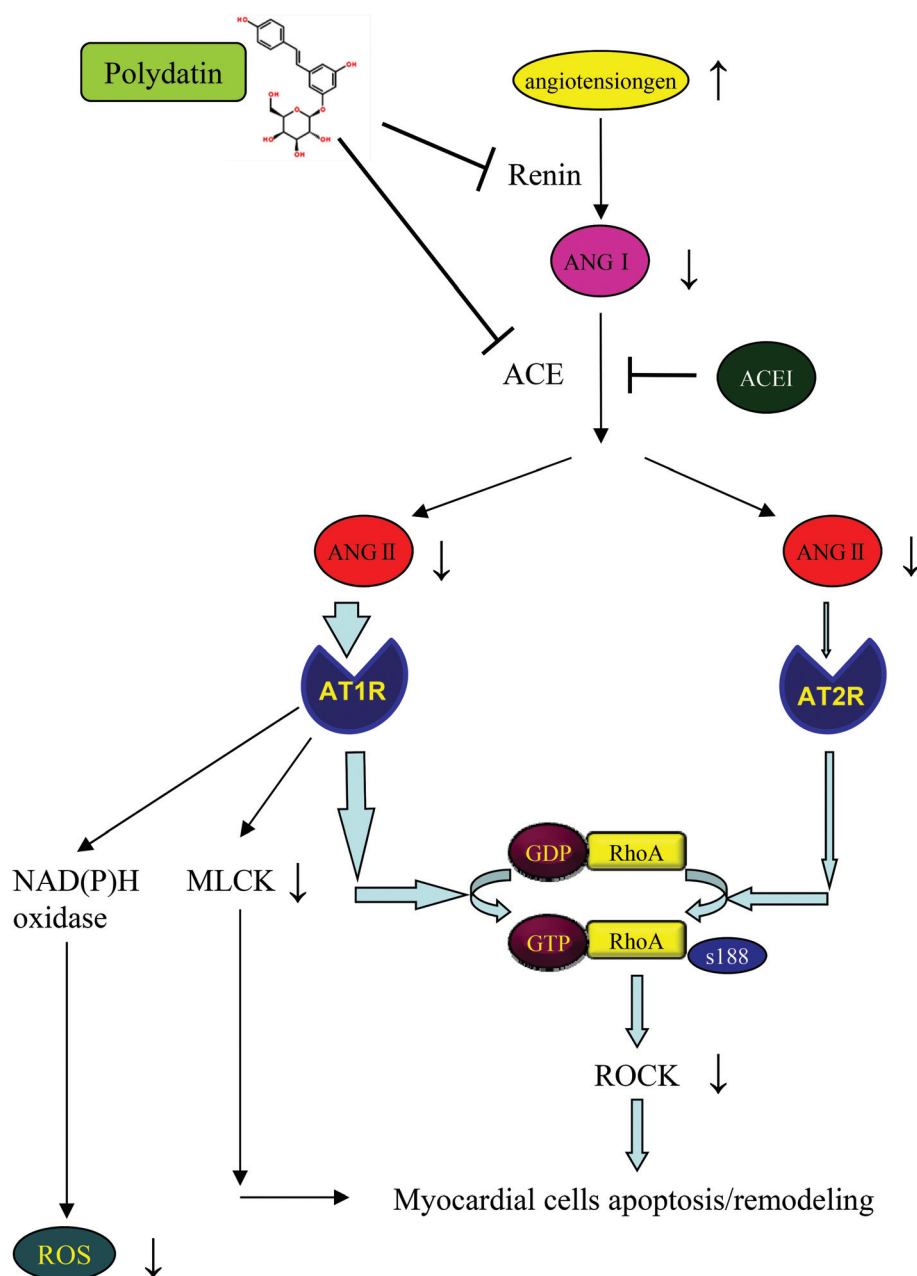


Fig. 8 Schematic representation of the protective effect of *trans*-polydatin on IR injury via inhibition of the RAS and downstream RhoA/ROCK pathway. PD inhibited the activity of rennin and ACE to reduce the content of ANG II, preventing the detrimental effect of AT1R mediated ROCK activation (shown in this study), as well as MLCK activation and ROS production (reported in previous studies). ROCK, Rho kinase; ACE, angiotensin-converting enzyme; AT1R, angiotensin receptor type 1; AT2R, angiotensin receptor type 2; ANG, angiotensin; ROS, reactive oxygen species.

AT2R was discovered to target at different parts of the ROCK pathway and play different roles from what has been known. The activated AT2R has been reported to specifically phosphorylate RhoA at the site of ser188, counteracting the ROCK-induced cardiac injury. Therefore, the balance between AT1R and AT2R might be associated with the regulation of the RAS during cardiac injury. After cardiac IR injury, AT1R and AT2R were observed to be up-regulated. Notably, the AT1R was found to induce major detrimental effects. In the study, with PD treatment, the expressions of AT1R and AT2R were decreased. However, during the further analysis, we noticed that PD exerted a more effective inhibition in AT1R expression and its downstream Rho/ROCK pathway than on AT2R expression and AT2R-mediated RhoA phosphorylation (ser188). For its potent protection against the major harm, PD might be superior to other ROCK inhibitors in treating the ROCK-related heart disease. The possible mechanism of the therapeutic function of PD during IR-induced cardiac injury is illustrated in Fig. 8. In our previous study, we discovered that orally administered *trans*-polydatin with a daily dose of 50 mg kg⁻¹ caused a protective effect in mice against the cardiac hypertrophy induced by transverse aortic constriction, and thus could be a potential treatment for cardiac hypertrophy.³⁴ Moreover, in this study, we found that orally administered PD with a safe dosage decreased the infarct size, attenuated myocardial fibrosis and apoptosis, and effectively increased the cardiac function in IR-injured mice. This *in vivo* trial highlights the important clinical function of PD in the treatment of cardiac IR injury.

In summary, this study confirms a strong cardio-protective effect of PD against IR injury. We demonstrate for the first time that PD inhibits both the local and circulating RAS by regulating renin and ACE, and therefore, is considered to be a potent substitute for ACEi and ARB to avoid the side effects. Furthermore, our study reveals further the causal relationship between the PD-induced inhibition of the RAS and the PD-induced inhibition of activated RhoA/ROCK, the former of which is highly responsible for the latter (Fig. 8). These findings thus underscore PD as a potential therapeutic strategy to optimally treat IR injury.

Limitation

In this study, polydatin was added to cells before IR *in vitro*. However, it was administered to mice after IR. *In vitro* and *in vivo* approaches should match. This should be explored further. Another limitation of this study is using neonatal cardiomyocytes as the *in vitro* model. It would be interesting to examine the effects of polydatin on adult cardiomyocytes subjected to IR in future studies.

Funding

This work was supported by grants from the National Natural Science Foundation of China (81202529 to M. D., 31371159 to J. L.).

Disclosure statement

None.

Compliance with ethical standards

The author Ming Dong has no conflict of interest to declare. The author Songyan Liao has no conflict of interest to declare. The author Zhaowen Xiao has no conflict of interest to declare. The author Ye Liu has no conflict of interest to declare. The author Na Zheng has no conflict of interest to declare. The author Jing Ma has no conflict of interest to declare. The author Wa Ding has no conflict of interest to declare. The author Jie Liu has no conflict of interest to declare.

All applicable international, national, and/or institutional guidelines for the care and use of animals were followed.

References

- 1 Y. Cheng, H. T. Zhang, L. Sun, S. Guo, S. Ouyang, Y. Zhang and J. Xu, Involvement of cell adhesion molecules in polydatin protection of brain tissues from ischemia-reperfusion injury, *Brain Res.*, 2006, **1110**, 193–200.
- 2 S. Zhou, R. Yang, Z. Teng, B. Zhang, Y. Hu, Z. Yang, M. Huan, X. Zhang and Q. Mei, Dose-dependent absorption and metabolism of *trans*-polydatin in rats, *J. Agric. Food Chem.*, 2009, **57**, 4572–4579.
- 3 L. P. Zhang, C. Y. Yang, Y. P. Wang, F. Cui and Y. Zhang, Protective effect of polydatin against ischemia/reperfusion injury in rat heart, *Sheng Li Xue Bao/Acta Physiol. Sin.*, 2008, **60**, 161–168.
- 4 L. P. Zhang, H. J. Ma, H. M. Bu, M. L. Wang, Q. Li, Z. Qi and Y. Zhang, Polydatin attenuates ischemia/reperfusion-induced apoptosis in myocardium of the rat, *Sheng Li Xue Bao/Acta Physiol. Sin.*, 2009, **61**, 367–372.
- 5 K. S. Zhao, C. Jin, X. Huang, J. Liu, W. S. Yan, Q. Huang and W. Kan, The mechanism of Polydatin in shock treatment, *Clin. Hemorheol. Microcirc.*, 2003, **29**, 211–217.
- 6 X. Wang, R. Song, Y. Chen, M. Zhao and K. S. Zhao, Polydatin—a new mitochondria protector for acute severe hemorrhagic shock treatment, *Expert Opin. Invest. Drugs*, 2013, **22**, 169–179.
- 7 Q. Miao, S. Wang, S. Miao, J. Wang, Y. Xie and Q. Yang, Cardioprotective effect of polydatin against ischemia/reperfusion injury: roles of protein kinase C and mito K(ATP) activation, *Phytomedicine*, 2011, **19**, 8–12.
- 8 W. Dai and R. A. Kloner, Potential role of renin-angiotensin system blockade for preventing myocardial ischemia/reperfusion injury and remodeling after myocardial infarction, *Postgrad. Med.*, 2011, **123**, 49–55.
- 9 S. Voros, Z. Yang, C. M. Bove, W. D. Gilson, F. H. Epstein, B. A. French, S. S. Berr, S. P. Bishop, M. R. Conaway, H. Matsubara, R. M. Carey and C. M. Kramer, Interaction between AT1 and AT2 receptors during postinfarction left

- ventricular remodeling, *Am. J. Physiol. Heart Circ. Physiol.*, 2006, **290**, H1004–H1010.
- 10 E. Kaschina, D. Lauer, P. Schmerler, T. Unger and U. M. Steckelings, AT₂ receptors targeting cardiac protection post-myocardial infarction, *Curr. Hypertens. Rep.*, 2014, **16**, 441.
 - 11 B. T. Andresen, K. Shome, E. K. Jackson and G. G. Romero, AT₂ receptors cross talk with AT₁ receptors through a nitric oxide- and RhoA-dependent mechanism resulting in decreased phospholipase D activity, *Am. J. Physiol. Renal Physiol.*, 2005, **288**, F763–F770.
 - 12 C. Guilluy, M. Rolli-Derkinderen, L. Loufrani, A. Bourge, D. Henrion, L. Sabourin, G. Loirand and P. Pacaud, Ste20-related kinase SLK phosphorylates Ser188 of RhoA to induce vasodilation in response to angiotensin II Type 2 receptor activation, *Circ. Res.*, 2008, **102**, 1265–1274.
 - 13 B. I. Jugdutt and V. Menon, AT₁ receptor blockade limits myocardial injury and upregulates AT₂ receptors during reperfused myocardial infarction, *Mol. Cell. Biochem.*, 2004, **260**, 111–118.
 - 14 J. Divisova, H. Vavrinkova, M. Tutterova, L. Kazdova and E. Meschisvili, Effect of ACE inhibitor captopril and L-arginine on the metabolism and on ischemia-reperfusion injury of the isolated rat heart, *Physiol. Res./Academia Scientiarum Bohemoslovaca*, 2001, **50**, 143–152.
 - 15 K. Horky, Does the rennin inhibitor aliskiren offer promising novel opportunities in the treatment of cardiovascular diseases?, *Vnitr. Lek.*, 2007, **53**, 364–370.
 - 16 W. Ding, M. Dong, J. Deng, D. Yan, Y. Liu, T. Xu and J. Liu, Polydatin attenuates cardiac hypertrophy through modulation of cardiac Ca²⁺ handling and calcineurin-NFAT signaling pathway, *Am. J. Physiol. Heart Circ. Physiol.*, 2014, **307**, H792–H802.
 - 17 A. Naderi, K. M. Chia and J. Liu, Synergy between inhibitors of androgen receptor and MEK has therapeutic implications in estrogen receptor-negative breast cancer, *Breast Cancer Res.*, 2011, **13**, R36.
 - 18 P. Rivera, M. P. Ocaranza, S. Lavandero and J. E. Jalil, Rho kinase activation and gene expression related to vascular remodeling in normotensive rats with high angiotensin I converting enzyme levels, *Hypertension*, 2007, **50**, 792–798.
 - 19 Y. Sun, J. Zhang, J. Q. Zhang and K. T. Weber, Renin expression at sites of repair in the infarcted rat heart, *J. Mol. Cell. Cardiol.*, 2001, **33**, 995–1003.
 - 20 R. Bhindi, P. K. Witting, A. C. McMahon, L. M. Khachigian and H. C. Lowe, Rat models of myocardial infarction. Pathogenetic insights and clinical relevance, *Thromb. Haemostasis*, 2006, **96**, 602–610.
 - 21 O. Ertracht, E. Liani, N. Bachner-Hinenzon, O. Bar-Am, L. Frolov, E. Ovcharenko, H. Awad, S. Blum, Y. Barac, T. Amit, D. Adam, M. Youdim and O. Binah, The cardioprotective efficacy of TVP1022 in a rat model of ischaemia/reperfusion, *Br. J. Pharmacol.*, 2011, **163**, 755–769.
 - 22 W. Bao, E. Hu, L. Tao, R. Boyce, R. Mirabile, D. T. Thudium, X. L. Ma, R. N. Willette and T. L. Yue, Inhibition of Rho-kinase protects the heart against ischemia/reperfusion injury, *Cardiovasc. Res.*, 2004, **61**, 548–558.
 - 23 B. Redfors, Y. Shao and E. Omerovic, Myocardial infarct size and area at risk assessment in mice, *Exp. Clin. Cardiol.*, 2012, **17**, 268–272.
 - 24 F. Gao, E. Gao, T. L. Yue, E. H. Ohlstein, B. L. Lopez, T. A. Christopher and X. L. Ma, Nitric oxide mediates the antiapoptotic effect of insulin in myocardial ischemia-reperfusion: the roles of PI3-kinase, Akt, and endothelial nitric oxide synthase phosphorylation, *Circulation*, 2002, **105**, 1497–1502.
 - 25 M. Dong, J. K. Liao, B. Yan, R. Li, M. Zhang and C. M. Yu, A combination of increased Rho kinase activity and N-terminal pro-B-type natriuretic peptide predicts worse cardiovascular outcome in patients with acute coronary syndrome, *Int. J. Cardiol.*, 2013, **167**, 2813–2819.
 - 26 B. Yang, D. Li, M. I. Phillips, P. Mehta and J. L. Mehta, Myocardial angiotensin II receptor expression and ischemia-reperfusion injury, *Vasc. Med.*, 1998, **3**, 121–130.
 - 27 F. M. Tavares, I. B. da Silva, D. A. Gomes and M. L. Barreto-Chaves, Angiotensin II type 2 receptor (AT₂R) is associated with increased tolerance of the hyperthyroid heart to ischemia-reperfusion, *Cardiovasc. Drugs Ther.*, 2013, **27**, 393–402.
 - 28 A. Abbate, G. G. Biondi-Zoccai and A. Baldi, Pathophysiologic role of myocardial apoptosis in post-infarction left ventricular remodeling, *J. Cell. Physiol.*, 2002, **193**, 145–153.
 - 29 J. C. Ferreira, A. V. Bacurau, F. S. Evangelista, M. A. Coelho, E. M. Oliveira, D. E. Casarini, J. E. Krieger and P. C. Brum, The role of local and systemic renin angiotensin system activation in a genetic model of sympathetic hyperactivity-induced heart failure in mice, *Am. J. Physiol. Regul. Integr. Comp. Physiol.*, 2008, **294**, R26–R32.
 - 30 V. G. Athyros, D. P. Mikhailidis, A. I. Kakafika, K. Tziomalos and A. Karagiannis, Angiotensin II reactivation and aldosterone escape phenomena in renin-angiotensin-aldosterone system blockade: is oral renin inhibition the solution?, *Expert Opin. Pharmacother.*, 2007, **8**, 529–535.
 - 31 W. C. De Mello, Intracellular Renin Disrupts Chemical Communication between Heart Cells. Pathophysiological Implications, *Front. Endocrinol.*, 2014, **5**, 238.
 - 32 R. B. Silver, A. C. Reid, C. J. Mackins, T. Askwith, U. Schaefer, D. Herzlinger and R. Levi, Mast cells: a unique source of renin, *Proc. Natl. Acad. Sci. U. S. A.*, 2004, **101**, 13607–13612.
 - 33 B. Yang, J. J. Li, J. J. Cao, C. B. Yang, J. Liu, Q. M. Ji and Z. G. Liu, Polydatin attenuated food allergy via store-operated calcium channels in mast cell, *World J. Gastroenterol.*, 2013, **19**, 3980–3989.
 - 34 M. Dong, W. Ding, Y. Liao, Y. Liu, D. Yan, Y. Zhang, R. Wang, N. Zheng, S. Liu and J. Liu, Polydatin prevents hypertrophy in phenylephrine induced neonatal mouse cardiomyocytes and pressure-overload mouse models, *Eur. J. Pharmacol.*, 2015, **746**, 186–197.